Available online at www.sciencedirect.com
ScienceDirect
Physica E 37 (2007) 138–141
PHYSICA E
www.elsevier.com/locate/physe

Catalytic and seeded shape-selective synthesis of II–VI semiconductor nanowires

A. Fasoli[a,*], A. Colli[a], S. Kudera[b], L. Manna[b], S. Hofmann[a], C. Ducati[c], J. Robertson[a], A.C. Ferrari[a]

[a]*Engineering Department, Cambridge University, Cambridge CB3 OFA, UK*
[b]*National Nanotechnology Laboratory, Lecce, Italy*
[c]*Department of Materials Science and Metallurgy, Cambridge University, Cambridge CB2 3QZ, UK*

Available online 6 September 2006

Abstract

We demonstrate catalytic and seeded shape-selective growth of CdSe nanostructures by a steady-state vapor-transport process. By varying the powder and sample temperatures, we observe a transition from a regime where catalytic growth is dominant to a metal-free self-induced nucleation regime. We then show that the best structural and optical quality are obtained by using CdSe colloidal nanocrystals as seeds for metal-free growth, as indicated by electron microscopy, X-ray diffraction and photoluminescence.

PACS: 61.46.−w

Keywords: Cdse; Nanostructures; Vapor transport; Colloids

1. Introduction

High-aspect-ratio semiconductor nanostructures are of great interest due to their potential applications in electronics and photonics [1–3]. II–VI materials, in particular, can be grown in a variety of different shapes such as nanowires (NWs), nanoribbons (NRs), nanosaws (NSs), nanorods (NRDs) or multi-branched structures [4–7]. Vapor-phase deposition techniques usually involve the use of a metal catalyst particle to promote NW nucleation [1,2,6–8]. Within this approach, however, the metal may result in a source of contamination, leading to the formation of detrimental scattering centers and intra-bandgap deep-level states [9].

Vapor transport in a single-zone quartz tube furnace is a widely employed approach for nanostructure synthesis [6,7,10,11]. Several groups reported catalyst-free NWs or NRDs by this technique [6,10,12]. In some cases, it was claimed that homo- or hetero-epitaxial nucleation on pre-existing crystalline surfaces was needed as a driving force for NRD growth [6,12], although similar results were also obtained on amorphous substrates [10]. On the other hand, wet-chemistry also allows metal-free synthesis of NRDs in solution [4,13]. Their dimensions, though, do not exceed a few hundreds nanometers, limiting their potential for some applications. Also, they cannot be selectively grown and aligned on a substrate in well-defined positions, but require post-deposition handling.

CdSe is one of the most investigated II–VI semiconductors [4,6]. With its bulk direct bandgap of 1.73 eV, it is a very promising candidate for photovoltaics applications. Here we identify three different growth regimes for CdSe nanostructures synthesis: catalytic, self-seeded and colloid-seeded growth. We then report the catalyst-free synthesis of CdSe NRDs and multipods by vapor transport.

2. Experimental

CdSe nanostructures are synthesized by vapor transport in a horizontal tube, single-zone furnace reactor. Key features of our system and synthesis procedures are

*Corresponding author. Tel.: +44 1223 748377; fax: +44 1223 748348.
E-mail addresses: af343@hermes.cam.ac.uk (A. Fasoli), acf26@eng.cam.ac.uk (A.C. Ferrari).

1386-9477/$ - see front matter © 2006 Elsevier B.V. All rights reserved.
doi:10.1016/j.physe.2006.06.010

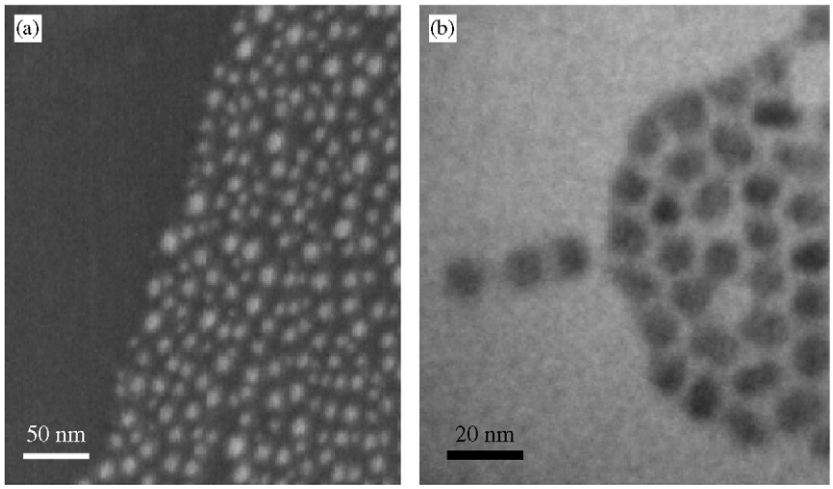

Fig. 1. (a) FEGSEM image of Au nanoislands resulting from the splitting of the patterned catalyst layer. (b) TEM image of CdSe colloids used for colloid-assisted growth [13].

described elsewhere [8]. For the set of experiments described here, we use Au-patterned (0.5 nm) oxidized Si ⟨1 0 0⟩ substrates for catalytic NW growth. During the heating ramp, the catalyst layer splits into nanoislands about 10 nm in diameter, as shown in Fig. 1(a). Bare-oxidized Si ⟨1 0 0⟩ chips are used for seeded growth. CdSe nanocrystals (5–10 nm in diameter), produced by solution methods [14] are dispersed from chloroform onto oxidized Si substrates for colloid-assisted growth (Fig. 1(b)). CdSe nanostructures are characterized by field-emission-gun scanning electron microscopy (FEGSEM), transmission electron microscopy (TEM), X-ray diffraction (XRD) and photoluminescence (PL). PL measurements are acquired by using an Ar-ion laser coupled to a micro-Raman spectrometer.

3. Results and discussion

We previously demonstrated that Au-catalyzed shape-selective synthesis of CdSe nanostructures is ruled by an interplay between surface kinetics and precursor impinging rate [8]. For our vapor-transport furnace reactor, these two parameters are driven by substrate and powder temperature, respectively (T_S, T_P). The lower triangle of the diagram in Fig. 2 summarizes the general trends observed for NW, NR and NS synthesis [8,15]. The main idea behind position and shape selectivity relies on the different CdSe vapor sticking and kinetics on different surfaces. In our particular case, interactions between $CdSe_{(V)}$–Au, $CdSe_{(V)}$–$CdSe_{(S)}$, and $CdSe_{(V)}$–$SiO_{2(S)}$ (V = vapor, S = solid) have to be considered. Due to the higher sticking coefficient of CdSe on Au, Au-catalyzed NWs can be grown, with no excess CdSe deposited on the NW sidewalls or on the uncoated SiO_2 areas of the substrate (Fig. 2, lower vertex). At higher powder temperatures, however, the thermal energy is no longer sufficient to fully desorb the incoming precursor. Thus homoepitaxial CdSe growth occurs on the NW sidewalls, leading eventually to a NR or NS

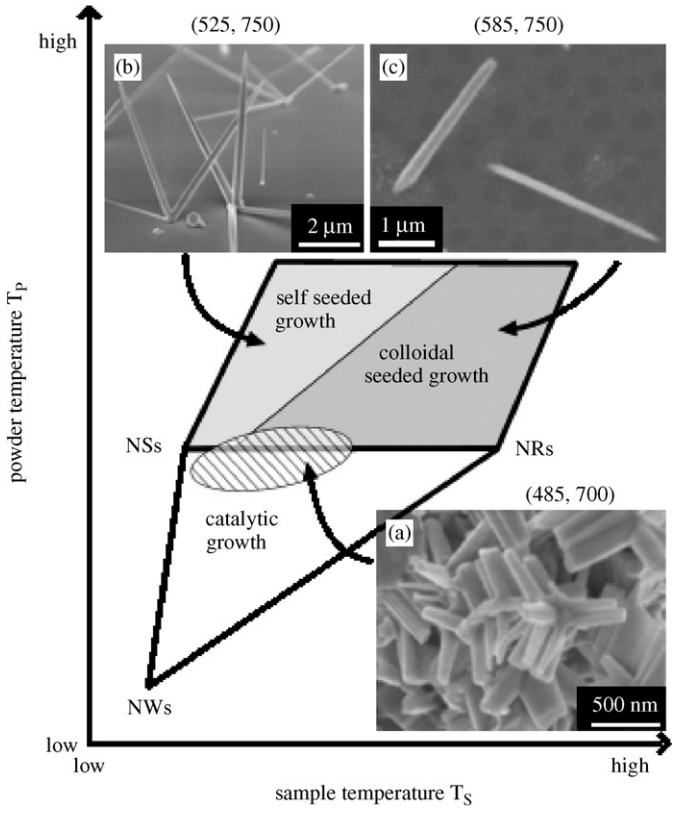

Fig. 2. Shape diagram of CdSe nanostructures obtained by varying powder and sample temperatures. Three growth regimes are found.

morphology (Fig. 2). Hence, a proper combination of parameters allows us to control the nanocrystal shape [8]. It should be noted that, within the NWs–NRs–NSs region of Fig. 2, position selectivity can always be achieved by pattering the Au catalyst. This because the sticking of CdSe vapor on SiO_2 is still suppressed for these conditions [8,16].

Within the NS regime ($T_P > 650\,^{\circ}C$, $450\,^{\circ}C < T_S < 500\,^{\circ}C$), elongated NRD branches begin to form on Au-catalyzed

NWs or NRs (Fig. 2(a)) [8]. This indicates that Au-free CdSe NRDs may be synthesized at higher T_P compared to their Au-catalyzed NW counterpart, though still requiring an existing CdSe surface to promote initial nucleation. By further increasing T_P, however, the local CdSe vapor density becomes enough for CdSe nanoislands to nucleate even on the bare SiO_2 substrate. This is the regime marked as self-seeded growth in Fig. 2. For such a combination of parameters, it is possible to grow nanopods and NRDs on bare-oxidized Si chips, without the need of any metal catalyst or surface preparation (Fig. 2(b)). In fact, two separate mechanisms take place in a self-seeded process. The first is the nucleation of a CdSe seed on SiO_2. For fixed T_P, a higher density of seeds is achieved by *lowering* T_S. Then, as soon as the seed is formed, this constitutes a preferential sticking point to promote further anysotropic epitaxial growth, similar to what happens for a NS teeth. However, we find that the formation of regular rods versus multipods or more disordered structures is enhanced by *increasing* T_S (for fixed T_P). The overlap between seed formation and NRDs growth is thus very narrow and a compromise has to be reached between final density and morphology of the resulting nanostructures.

In order to overcome these limitations, we decouple NRD growth and seed preparation by dispersing spherical CdSe colloidal nanocrystals on Si chips prior to loading the substrates in the vapor-transport reactor. In this case, initial condensation of CdSe vapor on SiO_2 is no longer necessary and NRD formation can be achieved at higher T_S compared to self-seeded growth (Fig. 2, colloidal-seeded growth region). The best uniformity in terms of NRD morphology, length and diameter is found by following this approach (Fig. 2(c)). In addition, colloid-seeded NRDs tend to exhibit a spontaneous vertical alignment.

XRD measurements performed on self-seeded multipods (Fig. 1(b)) and colloid-seeded NRDs are shown in Fig. 3. Several powder-diffraction peaks are detected for the self-seeded sample, which can be assigned both to cubic and hexagonal CdSe (Fig. 3(a)). A single phase (wurtzite) is revealed by the 2θ scan in Fig. 3(b) instead. Peaks related to Cd oxides (marked as '*' in Fig. 3) are seen in both cases, probably due to post-growth surface oxidation when exposing the samples to atmosphere. XRD results indicate that NRDs grown at higher T_S by means of colloidal seeds also offers a superior crystallographic quality. It has been reported that CdSe tetrapods grown by solution-based techniques exhibit a zinc blende (cubic) core and wurtzite (hexagonal) branches [13]. However, there is also evidence that such proposed dual-phase nucleation is not responsible for tetrapods formation but rather this is triggered by the presence of crystal twinnings within the wurtzite tetrapod core [17]. Due to the wide shape distribution of our self-seeded nanostructures, we believe that the mixed phase detected in Fig. 3(a) accounts more for highly disordered crystals rather than for regular cubic-core/wurzite-branch tetrapods. On the other hand, colloidal nanocrystals guarantee a much better seed uniformity, both in terms of shape and size distribution. As an additional advantage, we emphasize

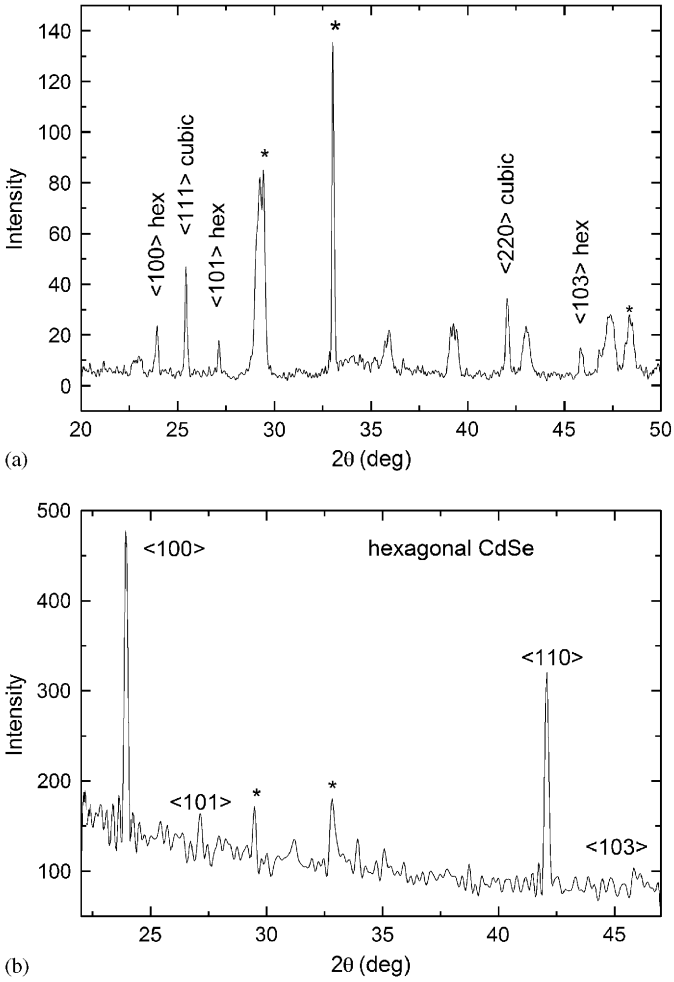

Fig. 3. XRD spectra comparing the internal structure of (a) self-seeded CdSe multi-branched nanostructures, presenting both zinc blende (cubic) and wurtzite (hexagonal) phases and (b) colloid-assisted CdSe NRDs, where wurtzite phase is dominant. Peaks labeled by '*' are assigned to CdO_2 [17].

that colloidal seeds might be pre-patterned ex situ on Si substrates by means of various techniques [4,18], whereas the in situ self-seeding process occurs randomly on the surface with no possible selective placement.

Finally, Fig. 4 compares the temperature-dependent optical emission of Au-catalyzed CdSe NWs and colloid-seeded CdSe NRDs. PL spectra in Fig. 4(a) show a broad and structured low-energy emission band around 1.7 eV, which may be attributed to electron-to-shallow-acceptor and shallow-donor-to-acceptor transitions [19]. Compared to the near-band-edge emission, such band is dominant at low temperatures and disappears above 170 K, as expected [19]. No low-energy band is found for the NRDs in Fig. 4(b). The possibility for the Au catalyst being responsible for the differences in PL emission is currently under investigation.

As a final remark, we note that, unlike the CdSe colloids PL emission (Fig. 1), NBE emission of CdSe NWs and NRDs occurs at the bulk CdSe bandgap energy. No quantum confinement effects are observed as the Bohr radius for CdSe is as low as 5 nm [20] (our Au-catalyzed

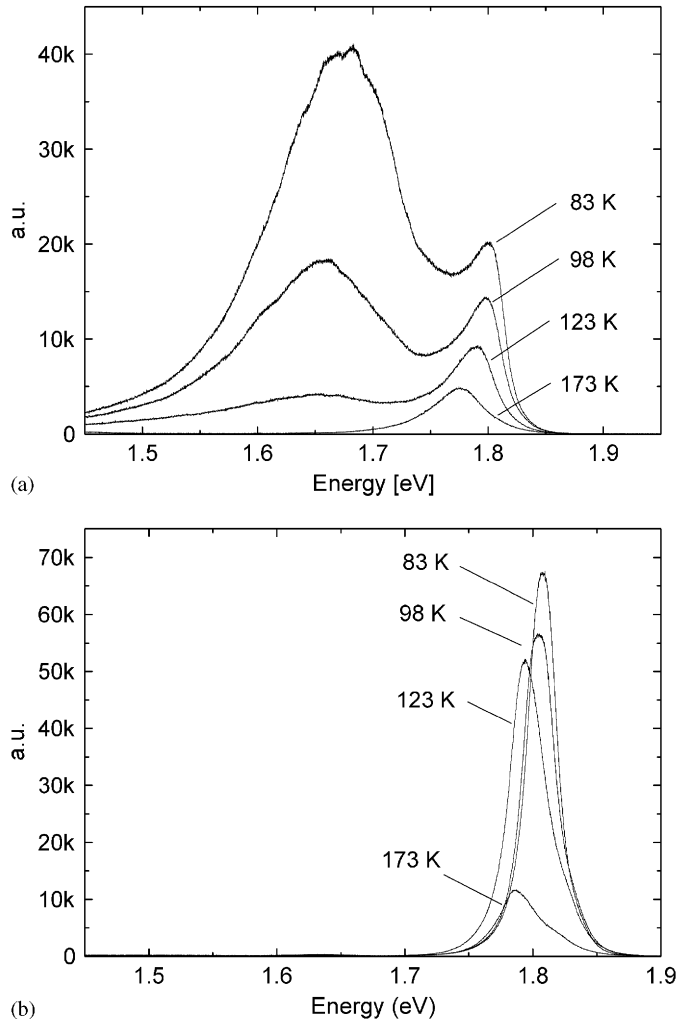

Fig. 4. PL spectra of (a) catalytically synthesized NRDs and (b) NRDs from colloid-assisted growth. No low-energy peaks associated to lattice defects or impurities are found for the colloid-assisted NRDs, suggesting their superior crystal quality.

NW are typically ~50 nm in diameter [8]). The NRD diameter (~100–200 nm) is also much larger than the size of the original CdSe colloids (5 nm). The dispersed nanocrystals act only as seeds to initiate NR formation, and do not appear to limit the NR diameter (as opposed to Au seeds for catalytic growth). In principle, *any* particle or material with higher sticking coefficient than SiO_2 could be potentially suitable for such purpose. However, by choosing nanocrystal seeds *made of the same material* as the NRDs we can rule out undesirable contamination. Self-driven anisotropic growth for catalyst-free NRDs is believed to arise from a combination of material-related properties (such as surface energy and polarity [10]) and experimental conditions [21].

4. Conclusion

In summary, we demonstrated the catalytic, self-seeded and colloidal-assisted growth of CdSe nanostructures by thermal evaporation in a single-zone furnace tube. Use of CdSe colloids made possible the metal-free homoepitaxial synthesis of NRDs in a high-T_P regime, overcoming this intrinsic self-seeded growth limitation. This solution provides the best NRDs in terms of uniformity of morphology, diameter, and length. Comparison of XRD spectra on self-seeded and colloidal-assisted grown nanostructures demonstrates the superior crystallographic quality of the high-T_P NRDs, which exhibit uniform hexagonal structural arrangement. Good optical quality was confirmed by low-temperature PL measurements.

Acknowledgements

AF acknowledges funds from ETRI, EPSRC, Cambridge European Trust and Pembroke College. ACF acknowledges funding from The Royal Society and The Leverhulme Trust. This work was supported by the Ministry of Information and Communication, Republic of Korea, under project No. A1100-0501-0073.

References

[1] M. Law, J. Goldberger, P. Yang, Annu. Rev. Mater. Res. 34 (2004) 83.
[2] X.F. Duan, Y. Huang, R. Agarwal, C.M. Lieber, Nature 421 (2003) 241.
[3] W.U. Huynh, J.J. Dittmer, A.P. Alivisatos, Science 295 (2002) 2425.
[4] L. Manna, D.J. Milliron, A. Meisel, E.C. Scher, A.P. Alivisatos, Nat. Mater. 2 (2003) 382.
[5] Z.L. Wang, Mater. Today 7 (2004) 26.
[6] C. Ma, Y. Ding, D. Moore, X. Wang, Z.L. Wang, J. Am. Chem. Soc. 126 (2004) 708.
[7] A. Colli, S. Hofmann, A.C. Ferrari, C. Ducati, F. Martelli, S. Rubini, S. Cabrini, A. Franciosi, J. Robertson, Appl. Phys. Lett. 86 (2005) 153103.
[8] A. Colli, A. Fasoli, S. Hofmann, C. Ducati, J. Robertson, A.C. Ferrari, Nanotechnology 17 (2006) 1046.
[9] P.J. Dean, B.J. Fitzpatrick, R.N. Bhargava, Phys. Rev. B 26 (1982) 2016.
[10] Z.R. Dai, Z.W. Pan, Z.L. Wang, Adv. Funct. Mater. 13 (2003) 9.
[11] D.D.D. Ma, C.S. Lee, F.C.K. Au, S.Y. Tong, S.T. Lee, Science 299 (2003) 1874.
[12] R.C. Wang, C.P. Liu, J.L. Huang, S.J. Chen, Appl. Phys. Lett. 86 (2005) 251104.
[13] L. Manna, E.C. Scher, A.P. Alivisatos, J. Am. Chem. Soc. 122 (2000) 12700.
[14] Z.A. Peng, X.G. Peng, J. Am. Chem. Soc. 123 (2001) 183.
[15] A. Fasoli, A. Colli, S. Hofmann, C. Ducati, J. Robertson, A.C. Ferrari, Phys. Status Solids, in press.
[16] D.P. Masson, D. Landheer, T. Quance, J.E. Hulse, J. Appl. Phys. 84 (1998) 4911.
[17] L. Carbone, S. Kudera, E. Carlino, W.J. Parak, C. Giannini, R. Cingolani, L. Manna, J. Am. Chem. Soc. 128 (2006) 748.
[18] R.A. McMillan, C.D. Paavola, J. Howard, S.L. Chan, N.J. Zaluzec, J.D. Trent, Nat. Mater. 1 (2002) 247.
[19] D.L. Rosen, Q.X. Li, R.R. Alfano, Phys. Rev. B 31 (1985) 2396.
[20] H. Fu, L.W. Wang, A. Zunger, Phys. Rev. B 59 (1999) 5568.
[21] V.B. Shenoy, Appl. Phys. Lett. 85 (2004) 2376.